

6 Results: SAXS & SANS

In the beginning of the experiment it was necessary to find out whether there was a damage of the sample due to the very intense synchrotron radiation. Such a damage would manifest itself in a change of the scattering pattern (e.g. due to the formation of aggregates). Thus, a sequence of spectra from solutions of DIMEB, β - and γ -CD was recorded; no indication of the sample damage was seen. A solution of TRIMEG was irradiated for 1 hour, and the subsequently recorded spectrum showed also no signs of radiation damage. Therefore, series of the spectra were recorded for a given solute concentration and for a number of different temperatures without refilling the sample cell with a fresh solution.

6.1 Scattering by dilute solutions

In the analysis of the SAXS spectra of the lowest concentrations studied (6 - 10.0 mg/mL), the concentration effects can presumably be neglected (i.e. $S_{\text{SOL}}(Q, c)$ can be set to unity), and these spectra represent, therefore, the scattering from the solution at infinite dilution, $I_{\text{EXP SAXS}}(Q)$. This approximation makes it possible to compare $I_{\text{EXP SAXS}}(Q)$ to $I_{\text{THEO SAXS}}(Q)$ computed from eq. (4.4), (see Fig. 6.1) and to characterize the form in which the molecules are present in solution (through evaluation of $R_{\text{g}}^2(\text{EXP})$, D_{EXP} , V_{EXP}).

For β - and γ -CD the agreement between experimental and computed scattering curves is good for $Q < 0.4 \text{ \AA}^{-1}$. For $Q > 0.4 \text{ \AA}^{-1}$, the scattering by the sample is nearly Q -independent and only slightly greater than the scattering by the cell filled with pure D_2O , so that in this region $I_{\text{EXP SAXS}}(Q, c)$ is somewhat uncertain for small solute concentrations, see eq. (4.1). For DIMEB and TRIMEG, however, the computed curves clearly differ from the experimental ones (Fig. 6.1c,d).

It is important to consider the dependence of the solute scattering intensity $I(Q)$ on the scattering contrast, $\Delta\rho_{\text{AV}}$. The well-known Debye formula states:

$$I(Q) = \int_V \int_V \Delta\rho(\mathbf{r}_1) \Delta\rho(\mathbf{r}_2) \frac{\sin Q|\mathbf{r}_1 - \mathbf{r}_2|}{Q|\mathbf{r}_1 - \mathbf{r}_2|} d\mathbf{r}_1 d\mathbf{r}_2 \quad (6.1)$$

where $\Delta\rho(\mathbf{r}) = \Delta\rho_{\text{AV}} + \rho_{\text{S}}(\mathbf{r})$ and $\rho_{\text{S}}(\mathbf{r})$ is the deviation of the solute electron density from the average value, ρ_{AV} , so that $\rho_{\text{S}}(\mathbf{r}) = \rho(\mathbf{r}) - \rho_{\text{AV}}$. Eq. (6.1) can be written as the sum of three terms:

$$I(Q) = (\Delta\rho_{\text{AV}})^2 \times I_0(Q) + 2 \times (\Delta\rho_{\text{AV}}) \times I_{01}(Q) + I_1(Q) \quad (6.2)$$

where $I_0(Q)$ is the so-called shape scattering, $I_{01}(Q)$ and $I_1(Q)$ are the terms due to deviations of the electron density from its average value. The theoretical scattering curve $I_{\text{THEO SAXS}}(Q)$ was evaluated in the frame of ‘‘homogeneous approximation’’; thus, $I_{\text{THEO SAXS}}(Q)$ is exactly the term

$I_0(Q)$ in eq. (6.2). For β - and γ -CD, judging by the good agreement between experimental and calculated scattering curves (see Fig. 6.1a,b), $I_0(Q)$ constitutes most of the scattering, i.e. the “homogeneous approximation” is valid for $Q < 0.5 \text{ \AA}^{-1}$.

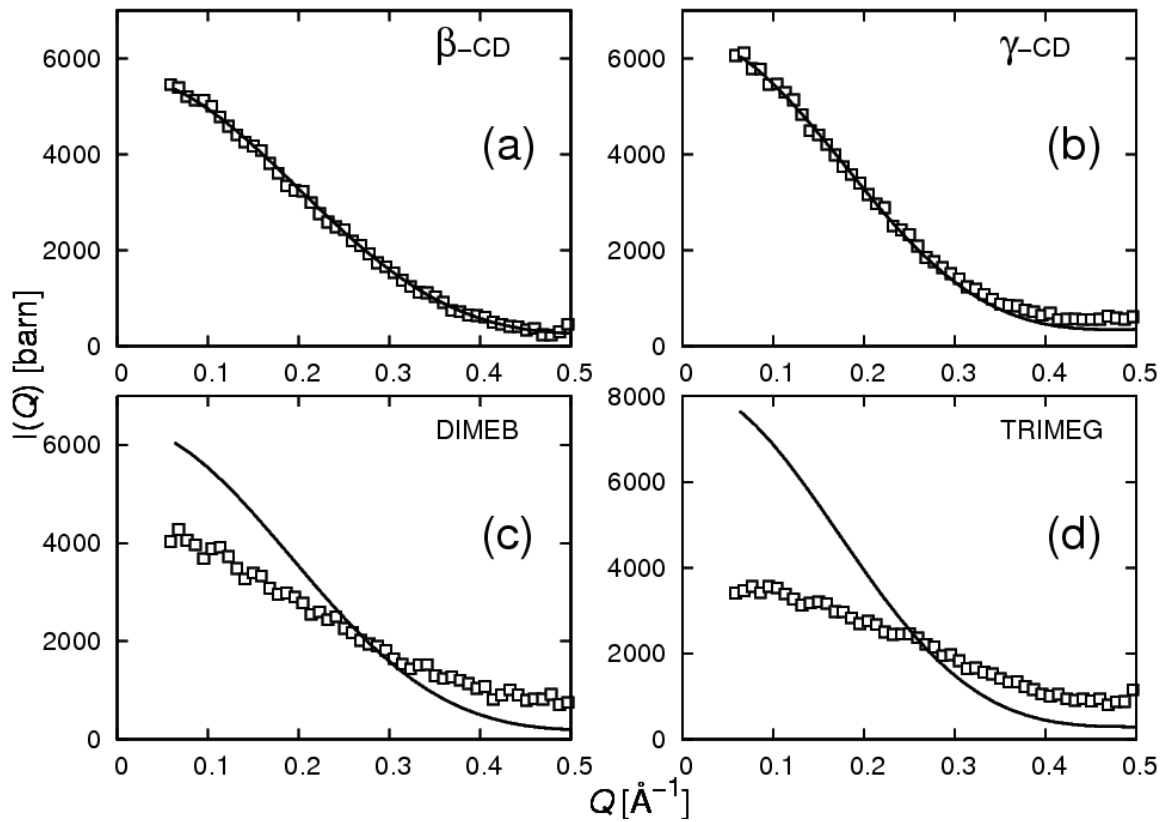


Figure 6.1 The comparison of the experimental, $I_{\text{EXP SAXS}}(Q)$, and theoretical, $I_{\text{THEO SAXS}}(Q)$, SAXS curves of D_2O solutions of CDs and mCDs. Legend: $I_{\text{EXP SAXS}}(Q)$ (\square); $I_{\text{THEO SAXS}}(Q)$ (—). (a): β -CD 7.1 mg/mL {6.2 mM}; (b): γ -CD 11.3 mg/mL {8.7 mM}; (c): DIMEB 6.6 mg/mL {5.0 mM}; (d): TRIMEG 10.0 mg/mL {6.1 mM}.

For mCDs, the poor agreement between $I_{\text{EXP SAXS}}(Q)$ and $I_{\text{THEO SAXS}}(Q)$ indicates that the terms $I_{01}(Q)$ and $I_1(Q)$ are likely to have substantial contribution to the total scattering curve. This is to be expected because the presence of methyl groups in DIMEB and TRIMEG results in a decrease of the average electron density (compared to β - and γ -CD, see Tab. 6.1) and, at the same time, in a greater variation of the electron density over the volume of the molecule. Indeed, the methyl group has as many electrons as one hydroxyl group, but occupies a larger volume. In the work of Bondi, van der Waals volumes of OH and CH_3 groups are given to be 8.04 and 13.67 cm^3/mole , respectively (Tabs. XV, XVI in [11]). But *the actual* increase of the volume, excluded by the solute, can be even larger.

$I_{01}(Q)$ and $I_1(Q)$ can be expanded in power series of Q with leading terms given by [120]:

$$I_{01}(Q) = V \times \alpha \times Q^2 \pm \dots \quad (6.3)$$

$$I_1(Q) = V \times \beta \times Q^2 \pm \dots \quad (6.4)$$

where V is the volume of the solute molecule. The parameters α and β are given by [120]:

$$\alpha = (1/V) \times \int \rho_S(\mathbf{r}) r^2 d\mathbf{r} \quad (6.5)$$

$$\beta = (1/V)^2 \times \int \rho_S(\mathbf{r}) \mathbf{r}_1 \mathbf{r}_2 d\mathbf{r}_1 d\mathbf{r}_2 \quad (6.6)$$

Since at low Q , $I_1(Q) = V \times \beta \times Q^2$ and for symmetrical molecules (like CDs and mCDs) the value of β is small; the term $I_1(Q)$ in eq. (6.2) can be neglected. One might expect that for mCDs the term $I_{01}(Q)$ is negative, because $I_{\text{EXP SAXS}}(Q) < I_{\text{THEO SAXS}}(Q)$ for low Q , see Fig. 6.1c,d. For mCDs, α evaluated from eq. (6.5) is negative (because the electron density is lower on the periphery due to the hydrogen atoms of the methyl groups) and thus $I_{01}(Q)$, determined from eq. (6.3), is negative, as expected.

Table 6.1 Average electron densities (ρ_{AV}) and contrast ($\Delta\rho_{\text{AV}}$) for CDs and mCDs; experimental and computed values of the square of gyration radius, maximum diameter of the solute molecule and volume estimate. Dimensions: ρ_{AV} and $\Delta\rho_{\text{AV}}$ [number of electrons/Å³]; R_g^2 [Å²], D [Å], V [Å³]; electron density of the solvent (D₂O) $\rho_0 = 0.3311$; $\Delta\rho_{\text{AV}} = \rho_{\text{AV}} - \rho_0$.

	ρ_{AV}	$\Delta\rho_{\text{AV}}$	$R_g^2(\text{EXP})$	$R_g^2(\text{THEO})$	D_{EXP}	D_{THEO}	V_{THEO}	V_{EXP}	N_d^b
β -CD	0.601	0.270	43.4 (1.20) ^a	39.6	18.7-20	17.7	1001	1127 (42) ^a	9
γ -CD	0.576	0.245	51.5(1.08) ^a	49.1	18.5-19.5	19.3	1195	1276 (40) ^a	7
DIMEB	0.557	0.226	30.0	43.4	16.7	19.8	1281	624	1
TRIMEG	0.531	0.200	20.1	53.3	10	22.4	1658	791	1

^a The standard deviation is given in parentheses.

^b N_d - number of experimental patterns used for the determination.

The curves $I_{\text{EXP SAXS}}(Q)$ of the dilute solutions were used to evaluate the square of the gyration radius, $R_g^2(\text{EXP})$, from eq. (4.6); the maximum diameter of the solute molecule, D_{EXP} , from eq. (4.5) and volume estimate, V_{EXP} , from eqs. (4.8, 4.9); the results are given in Tab. 6.1. The agreement between the computed and experimental values is good for β - and γ -CD and poor for DIMEB and TRIMEG.

The discrepancy observed for the square of gyration radius for DIMEB and TRIMEG can be explained considering its dependence on the contrast [120]:

$$R_g^2(\Delta\rho_{\text{AV}}) = R_g^2(\text{THEO}) + \alpha/\Delta\rho_{\text{AV}} - \beta/(\Delta\rho_{\text{AV}})^2 \quad (6.7)$$

Again, for symmetrical molecules the value of β is small, the term " $\beta/(\Delta\rho_{\text{AV}})^2$ " is therefore significant only for very small contrast and can be neglected in the present work. Because the contrast is positive (Tab. 6.1) and α is negative, the experimentally observed R_g^2 values are in the qualitative agreement with the theory. (The qualitative prove of the fact that α is negative for mCDs follows from the evaluation of α for two hollow concentric spheres, with the outer sphere having smaller electron density than the inner one.)

Since inhomogeneities in the distribution of the electron density are greater for

TRIMEG (all hydroxyl groups are methylated), than for DIMEB, the deviations of $R_g^2(\text{EXP})$ and $I_{\text{EXP SAXS}}(Q)$ from $R_g^2(\text{THEO})$ and $I_{\text{THEO SAXS}}(Q)$ are expected to be greater for TRIMEG. It is indeed the case, as can be seen from Fig. 6.1 and Tab. 6.1.

The experimental values of both the maximum diameter and the volume of the molecule are grossly underestimated for DIMEB and TRIMEG. This is not surprising, since eqs. (4.5) and (4.8) that were employed for the evaluation of D_{EXP} and V_{EXP} , respectively, are valid only within the Q -region where the shape scattering, $I_0(Q)$, dominates the total scattering intensity, $I(Q)$.

6.2 Existence of oligomers and/or aggregates in solutions of CDs and mCDs

Generally, a good agreement between the theoretical and experimental scattering curves is not sufficient to rule out the existence of aggregates in solutions of β - and γ -CD (although such agreement *does* rule out the presence of oligomers). It is the transformation of the spectra to the absolute scale that allows to prove unambiguously that there is no aggregation or crystallization, which would lead, effectively, to a decrease of the concentration of the monomeric form.

The spectra shown in Fig. 6.1 are on the absolute scale. Unfortunately, the scattering by the empty cell, I_{EC} , was not measured and the quantity $I_{\text{H}_2\text{O}}/I_{\text{EC}}$ (known from some previous measurements) can vary from one empty cell to the other. Thus, there is some uncertainty concerning the actual value of the factor $f_{\text{H}_2\text{O}}$ as determined from eq. (4.2). Therefore, the factor $f_{\text{H}_2\text{O}}$ was adjusted by ca. 10% to ensure that the experimental and theoretical SAXS curves for γ -CD overlap maximally. The so adjusted $f_{\text{H}_2\text{O}}$ was used for DIMEB and TRIMEG solutions, but for β -CD this factor had to be multiplied by 1.35 in order for $I_{\text{EXP SAXS}}(Q)$ to coincide with the corresponding theoretical curve. At room temperature, β -CD is poorly soluble in cold H_2O (18.5 mg/mL at 25 °C [53]), and there are no data on its solubility in D_2O . When a solution of β -CD in D_2O was prepared, some material remained undissolved, and the factor 1.35 is therefore most likely due to overestimated concentration of β -CD used in eq. (4.1). Thus, the actual concentration of β -CD was 5.26 mg/mL {4.6 mM}.

The results shown in Fig. 6.1 give evidence that β -CD, γ -CD, DIMEB and TRIMEG occur as monomers in aqueous solution under the studied conditions. Indeed, the existence of aggregates would result in a such drop of the monomeric concentration, that one would have $I_{\text{EXP SAXS}}(Q) < I_{\text{THEO SAXS}}(Q)$, but this is not the case (at least for $Q > 0.3 \text{ \AA}^{-1}$ for DIMEB and TRIMEG). The presence of oligomers in the solutions of DIMEB and TRIMEG would result in the steeper increase of $I_{\text{EXP SAXS}}(Q)$ towards low Q .

Regarding the formation of aggregates, it is important to note following: while the light

scattering (LS) study [22] claims the presence of aggregates for α -, β - and γ -CD, a later light scattering study [39] found no aggregates/oligomers for α -CD, γ -CD and DIMEB. Although they [39] reported the existence of aggregates for β -CD (1.3 mg/mL in H₂O), they could not determine the molecular mass for the latter. It is conceivable (considering the low solubility of β -CD in water and its low molecular mass and volume) that the apparently observed aggregates were merely due to some misinterpretation of the data.

6.3 Small-angle scattering and solute-solute interactions

Before the discussion of the concentration and temperature dependence of small-angle scattering spectra, it is appropriate to give the relevant information on the connection between the nature of the solute-solute interactions, SAXS and SANS spectra and the osmotic pressure.

The value of the intermolecular structure factor at the origin of reciprocal space, $S(0, c)$ is related to the osmotic pressure of the solution, Π , as follows:

$$S(0, c) = (RT/M) \times (\partial\Pi/\partial c)^{-1} \quad (6.8)$$

where R is the gas constant ($R = 8.31 \text{ mol}^{-1} \text{ K}^{-1}$), M is the molecular mass, c concentration [mg/mL]. The osmotic pressure can be expanded as a power series of the concentration:

$$\Pi/cRT = 1/M + A_2c + A_3c^2 + \dots \quad (6.9)$$

where A_2 , and A_3 are the second and the third virial coefficients, respectively. If the solute concentration is small and solute-solute interactions are weak, from eqs. (6.8, 6.9) it follows:

$$1/S(0, c) = 1 + 2M \times A_2 \times c \quad (6.10)$$

When solute-solute interactions are repulsive, the value of A_2 is positive, the osmotic pressure is higher than in the case when no solute-solute interactions exist and $S(0, c)$ is lower than unity. By contrast, if solute-solute interactions are attractive, A_2 adopts a negative value, rendering $S(0, c) > 1$. For protein solutions the value of A_2 is known to correlate with the solubility [43] (a decrease of A_2 corresponds to a decrease of solubility and *vice versa*).

As given by eq. (4.15), small-angle scattering intensity is the product of the particle scattering and the intermolecular structure factor. The structures of native and methylated cyclodextrin molecules in aqueous solution can be taken as virtually temperature and concentration independent; consequently, the same is true for the particle scattering. (Presumably, the eventual changes in the conformation of the glucose residues or -CH₂-OH groups (in CDs) and -OCH₃ & -CH₂-OCH₃ groups (in mCDs) will not lead to a substantial change of the particle scattering). From the discussion on $S(0, c)$ above (but this can be generally demonstrated too, see e.g. [99]) it follows that repulsive interactions manifest themselves in the small-angle X-ray and neutron scattering spectra through a decrease (and attractive interactions through an increase) of scattering intensity at low Q .

For the comparison of SAXS and SANS results with the results of osmotic pressure measurements, eq. (6.9) may be written as:

$$\Pi/\rho_{\text{SOLUTION}} = \varnothing \times \{c/(M \times \rho_{\text{SOLUTION}})\} \times RT \quad (6.11)$$

where ρ_{SOLUTION} is the density of the solution, $c/(M \times \rho_{\text{SOLUTION}})$ is the molality of the solute and \varnothing is the molal osmotic coefficient. Comparing eqs. (6.9) and (6.11), it is clear that in the ideal case (no interactions and virial coefficients are all zero), $\varnothing = 1$. If interactions are repulsive, $A_2 > 0$ and $\varnothing > 1$, in the case of attractive interactions $A_2 < 0$ and $\varnothing < 1$.

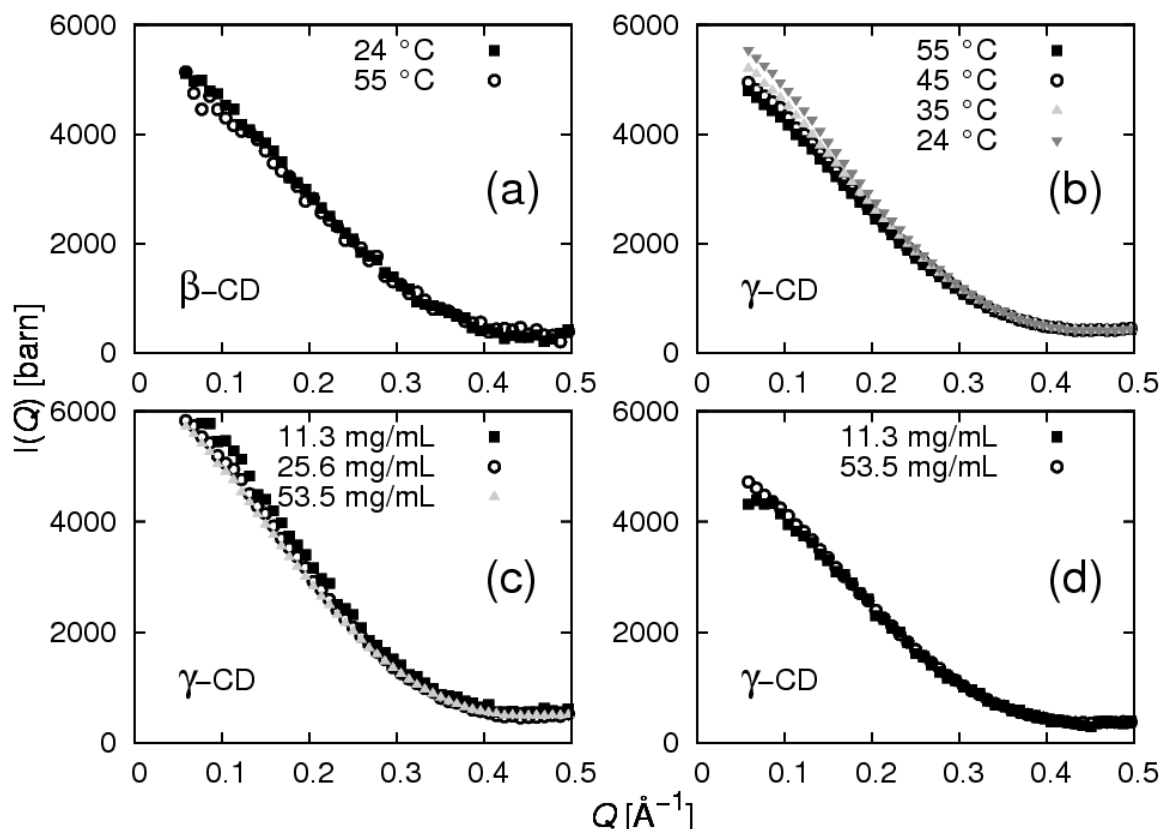


Figure 6.2 Temperature and concentration dependence of the experimental SAXS curves of β -CD and γ -CD solutions in D_2O . (a): β -CD 7.1 mg/mL {6.2 mM}; (b): γ -CD 53.5 mg/mL {41.3 mM}; (c): γ -CD at 24 °C; (d): γ -CD at 55 °C.

6.4 Concentration and temperature variation of the SAXS curves

Fig. 6.2 Owing to the low solubility of β -CD in water, only one concentration of β -CD was measured with SAXS in the temperature range 19 - 55 °C. A slight change of the scattering curve with temperature can be seen in Fig. 6.2a. Qualitatively, this change is in accord with an increase of the repulsive interactions at higher temperature. For γ -CD, the temperature dependence of SAXS is shown in Fig. 6.2b. The curve becomes steeper as the temperature decreases, meaning that interactions become more attractive, in accord with the fact

that γ -CD has a positive temperature coefficient of solubility in water. Figure 6.2c,d show the concentration dependence of $I_{\text{EXP SAXS}}(Q)$ for γ -CD. While at room temperature (24 °C) the scattering intensity decreases at low Q upon increase of concentration (indicating repulsive interactions), at 55 °C there is virtually no difference between the curves for 11.3 and 53.3 mg/mL {8.7 and 41.3 mM}.

Fig. 6.3 For DIMEB, an increase in both, temperature and concentration, leads to an increase in attractive interactions. As shown in Fig. 6.3a,b the scattering curve becomes more and more concave upon increase of the temperature. In Fig. 6.3c,d the increase of concentration leads to a strong increase of the scattering at low Q .

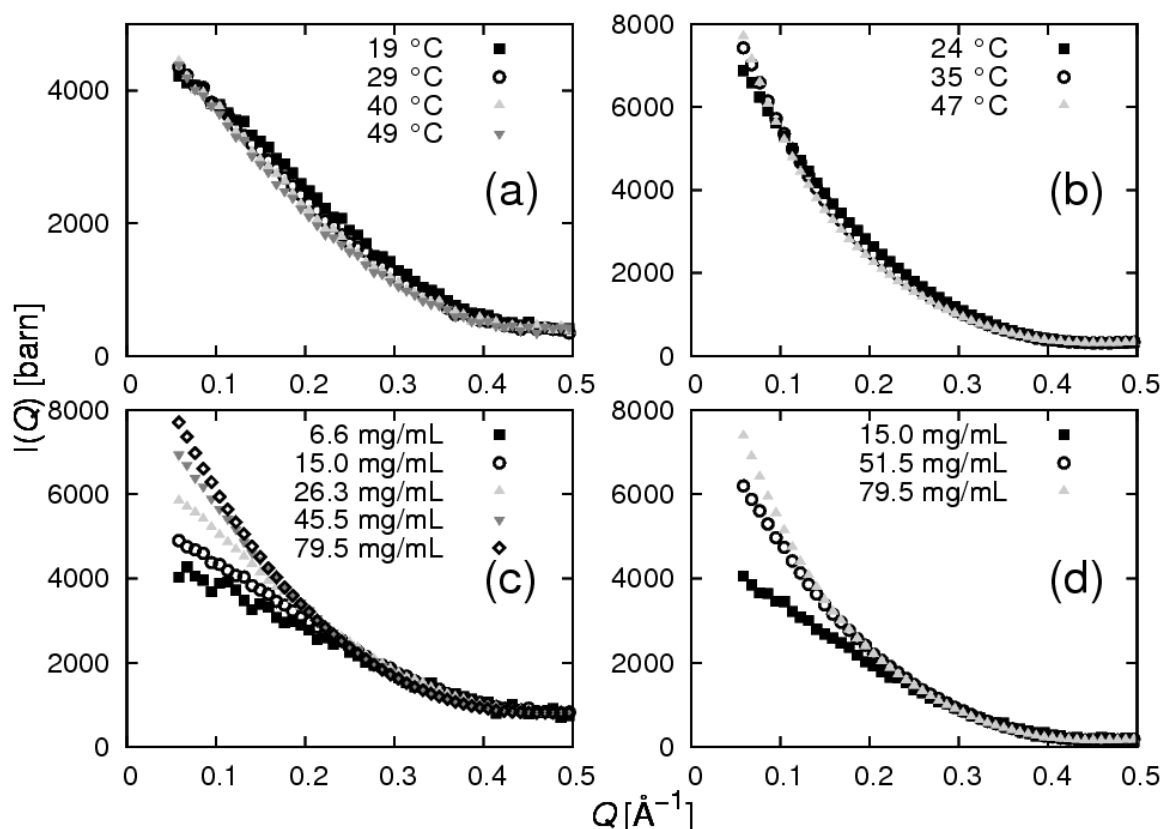


Figure 6.3 Temperature and concentration dependence of the experimental SAXS curves of DIMEB solutions in D_2O . (a): 15 mg/mL {11.3 mM}; (b): 79.5 mg/mL {59.8 mM}; (c): 24 °C except for 15.0 mg/mL measured at 19 °C; (d): 40 °C.

Fig. 6.4 For TRIMEG, the solute-solute interactions become more attractive with temperature: the scattering curve changes from convex at room temperature to increasingly concave upon temperature increase (Fig. 6.4a,b). At room temperature (24 °C) there is a decrease in the scattering intensity at low Q when the TRIMEG concentration increases (Fig. 6.4c), probably due to a corresponding increase in net repulsive interactions. (Such an interpretation can not explain why the scattering curve for $c=10$ mg/mL, lies below the curves for $c=17$ and 35.9 mg/mL for $Q < 0.3 \text{ \AA}^{-1}$.)

At 55 °C (Fig. 6.4d), the net interaction force is apparently only slightly repulsive or already attractive, so that the concentration dependence at this temperature becomes DIMEB-like, see Fig. 6.3a,b). Specifically, the curves for $c=35.9$, 66.7 and 95.4 mg/mL indicate an increase of the scattering in the low Q region, so that the curves become slightly more concave. (Note that the scattering curve for $c=17.0$ mg/mL contradicts the proposed explanation.)

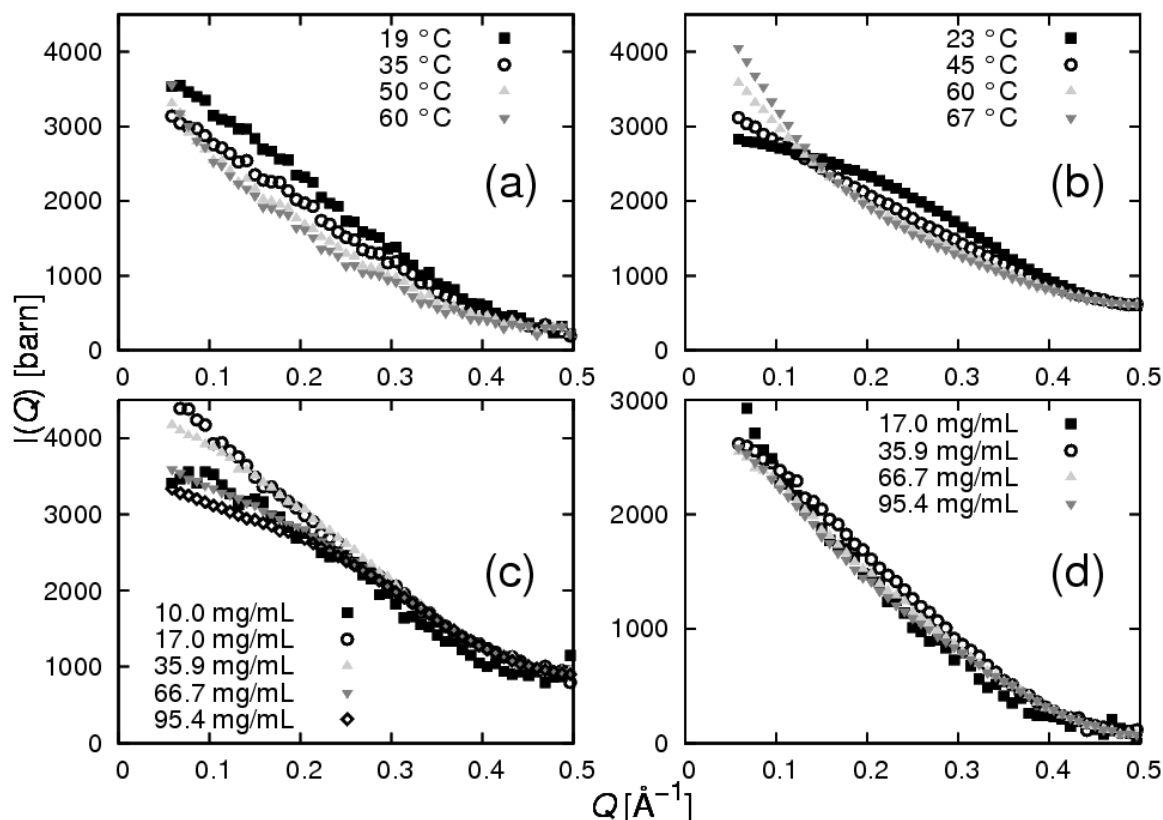


Figure 6.4 Temperature and concentration dependence of the experimental SAXS curves of TRIMEG solutions in D₂O. (a): 17 mg/mL {10.4 mM}; (b): 95.4 mg/mL {58.4 mM}; (c): at 24 °C; (d): at 55 °C.

Neglecting the inconsistencies admitted above for TRIMEG, the conclusion can be made as follows. While for DIMEB an increase in concentration leads to an increase in attractive interactions both at 24 and 40 °C (Fig. 6.3c,d), for TRIMEG it leads to an increase in repulsive interactions at 24 °C (Fig. 6.4c) whereas at 55 °C *no* increase in repulsive interactions is found (Fig. 6.4d). Such differences are in accord with the solubility of the two mCDs: at a concentration of 45.5 mg/mL {34.2 mM} in D₂O, DIMEB crystallizes at about 50-51 °C, whereas at 66.7 mg/mL {40.9 mM} in D₂O TRIMEG crystallizes at > 70 °C.

Regarding the TRIMEG scattering curve for $c=10.0$ mg/mL in Fig. 6.4c: the marked deviation of this curve from others in the region $Q>0.4$ Å⁻¹ suggests that either this particular sample scattering pattern or the subtracted D₂O pattern was biased. The same is probably true for the scattering curve $c=17.0$ mg/mL in Fig. 6.4d, where the abrupt increase of the scattering

intensity at low Q (first two points from the left) indicates that the sample cell was not clean.

It is important to stress that especially for a low CD or mCD concentration, the scattering curve (obtained by subtraction of the D_2O scattering pattern from the solution scattering pattern, see eq. (4.1)) was slightly different depending on the D_2O scattering pattern which was subtracted. Therefore, more work has to be done in order to confirm quantitatively very slight changes of the solute scattering curves with temperature or solute concentration found in the present study for β - and γ -CD, namely those in Fig. 6.2a and 6.2c,d.

6.5 *The SANS spectra of DIMEB and comparison with SAXS and osmotic pressure measurements*

The experimental SANS patterns of DIMEB, $I_{S/SANS}(Q)$, are shown in Fig. 6.5a,b. Generally, the trend is the same as found by SAXS: upon increase of temperature, the scattering intensity in the low Q region rises and then falls because of crystallization (not shown).

The theoretical SANS curve, $I_{THEO SANS}(Q)$, was evaluated from eqs. (4.10, 4.11); the scattering density of the solute molecule *was not* assumed to be homogeneous (as is the case for $I_{THEO SAXS}(Q)$) and it is therefore of great interest to compare theoretical and experimental SANS curves. The experimental SANS curves for different concentrations at 25 °C are shown together with $I_{THEO SANS}(Q)$ in Fig. 6.5c. The value of I_{INC} in eq. (4.14) was adjusted so that all curves overlap at $Q \approx 0.3 \text{ \AA}^{-1}$ (this kind of “shift” takes into account (somewhat sample-dependent) incoherent background and is justified in view of the SAXS results for DIMEB, see Fig. 6.3c). The wider scatter of data points for $Q < 0.1 \text{ \AA}^{-1}$ is due to a longer sample detector-distance used to record spectra in this Q region and consequently worse statistical accuracy. Qualitatively, the curves in Fig. 6.5c change with increasing concentration in a fashion similar to the one seen in Fig. 6.3c. The theoretical scattering curve is more gently sloping as opposed to the experimental (coherent) SANS curves suggesting that concentration effects may not be neglected even for the lowest DIMEB concentration, 6.6 mg/mL. Alternatively, it is possible that the observed difference is due to an underestimation of the excluded solvent volume in the evaluation of $I_{THEO SANS}(Q)$.

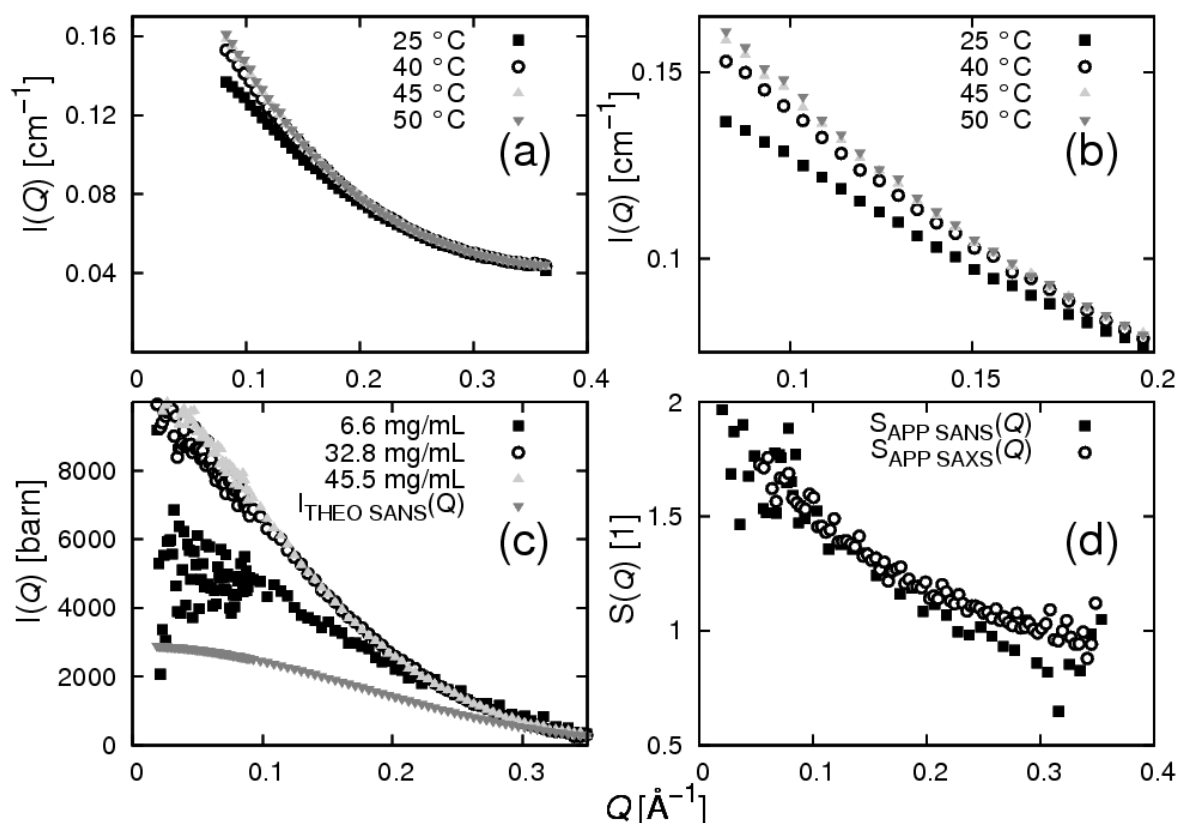


Figure 6.5 SANS results for DIMEB solutions in D₂O. **(a)**: temperature dependence of the experimental SANS patterns, $I_{S/SANS}(Q, c)$, for DIMEB solution in D₂O, $c=45.2$ mg/mL {34.0 mM}; **(b)**: the same as in **(a)**, magnified; **(c)**: Experimental SANS curves, $I_{EXP SANS}(Q, c)$, for various concentrations of DIMEB in D₂O at 25 °C and theoretical SANS curve of DIMEB (at infinite dilution), $I_{THEO SANS}(Q)$; **(d)**: the approximate structure factor $S_{APP SANS}(Q)$ and $S_{APP SAXS}(Q)$ for DIMEB solution in D₂O at 25 °C from SANS (■) and SAXS (○).

The ratios “ $I_{EXP SAXS}(Q, c=45.5)/I_{EXP SAXS}(Q, c=6.6)$ ” and “ $I_{EXP SANS}(Q, c=45.5) / I_{EXP SANS}(Q, c=6.6)$ ” (further denoted as $S_{APP SAXS}(Q, c=45.5)$ and $S_{APP SANS}(Q, c=45.5)$, respectively) are shown in Fig. 6.5d. Considering the scatter of the data points one may conclude that neutron and X-ray scattering give similar results.

The $S_{APP SANS}(Q)$ and $S_{APP SAXS}(Q)$ curves in Fig. 6.5d present the intermolecular structure factor for a given concentration, $S_{SOL}(Q, c=45.5)$, if concentration effects in 6.6 mg/mL solution of DIMEB can be indeed neglected (which essentially means setting $I(Q, c=6.6$ mg/mL) = $I(Q)$, see also eq. (4.15)). To find out whether this is so, small-angle scattering experiments on a series of dilute solutions would be required to obtain the scattering curve at infinite dilution. For such a purpose, SAXS seems to be more appropriate because the incoherent background is relatively high in SANS spectra of dilute DIMEB (and predictably other CDs and mCDs) solutions.

Measurements of the osmotic coefficients in aqueous solutions of α - and γ -CD [85] and

DIMEB [86] were reported. For α - and γ -CD, osmotic coefficients are slightly less than unity (about 0.97) for concentrations ≈ 50 mM indicating slight attractive interactions (see eqs. (6.9, 6.11)). In Fig. 6.2b some increase in the slope of the scattering curve of γ -CD also indicates increase of attractive interaction upon cooling, which may be taken as qualitative agreement with results [85]. However, the effect is rather small and should be studied more thoroughly.

Interestingly, osmotic coefficients measured for DIMEB [86] are substantially smaller than unity and decrease markedly both upon increase of the temperature and concentration, indicating an increase of attractive interactions and in agreement with SAXS and SANS results. For several DIMEB concentrations, the difference in the osmotic coefficient observed for 25 ° and 35 °C is higher, than this difference observed at 35 and 45 °C. This agrees with small-angle scattering results, especially well with SANS results, see Fig. 6.5b.

6.6 Determination of the second virial coefficient

The determination of $S_{\text{SOL}}(Q, c)$ at room temperature from eq. (4.15) was done as follows: $S_{\text{SOL}}(Q, c) = I_{\text{EXP SAXS}}(Q, c) / I_{\text{EXP SAXS}}(Q, c_{\text{min}})$, where c_{min} is 6.6 and 10 mg/mL for DIMEB and TRIMEG, respectively. By extrapolating $S_{\text{SOL}}(Q, c)$ to $Q=0$ and using eq. (6.10), the experimental values of the second virial coefficient, A_2 , for several concentrations of DIMEB and TRIMEG were found (see Tab. 6.2).

Table 6.2 Values of the second virial coefficient (A_2) for DIMEB and TRIMEG in D_2O at room temperature (24 °C) as function of concentration (determined from the experimental SAXS curves).

DIMEB		TRIMEG	
c [mg/mL]	A_2 [mol mL g ⁻²]	c [mg/mL]	A_2 [mol mL g ⁻²]
15	-0.00560	17	-0.00650
26.3	-0.00560	35.9	-0.00230
45.5	-0.00420	66.7	-0.00067
79.5	-0.00280	95.4	-0.00025

In the limit of validity of the linear approximation given by eq. (6.10) the value of A_2 must be independent of the solute concentration. The data in Tab. 6.2 indicate that both for DIMEB and TRIMEG the value of A_2 becomes less negative with increase of the concentration. It was attempted to determine A_2 values from the extended version of eq. (6.10) (by considering the next term in the power series of concentration):

$$1/S(0, c) = 1 + 2 \times M \times A_2 \times c + 3 \times M \times A_3 \times c^2 \quad (6.12)$$

where A_3 is the third virial coefficient. The so determined A_2 and A_3 values were not concentration independent either, therefore excluding a possible failure of eq. (6.10). For low

concentrations, the error in determining of $S(\theta, c)$ is larger than for the high concentration (see Figs. 6.3c and 6.4c for the concentration behavior of the SAXS curves). It is therefore plausible, that values of A_2 determined from the highest concentration are the most reasonable. This view is supported by the light scattering study [39] where they found A_2 for DIMEB to be 2.5×10^{-3} [mol mL g⁻²] at 25 °C in H₂O solution (it is not specified, for which DIMEB concentration(s) this value was obtained).

Note that a less negative value of A_2 for TRIMEG indicates less attractive solute-solute interactions in comparison with DIMEB.